Polarization effects of Nd^{3+} spectra in strontium hexa-aluminates

A. LUPEI, V. LUPEI*, C. GHEORGHE, L. GHEORGHE, E. ANTIC-FIDANCEV[a], D. VIVIEN[a], G. AKA[a]

Institute of Atomic Physics - INFLPR, 077125 Bucharest – Romania
[a]ENSCP, Lab. de Chimie Appliquée de l'Etat Solide, Paris, France

The disordered strontium hexa-aluminate crystals $Sr_{1-x}Nd_yLa_{x-y}Mg_xAl_{12-x}O_{19}$ (ASL) proved to be a system with a good potential for $^4F_{3/2} \rightarrow {}^4I_{9/2}$ laser emission at ~ 900 nm. There are two main different non-equivalent Nd^{3+} centers in disordered ASL crystals. New data on the symmetry of one the Nd^{3+} centers in ASL, prevailing at low x composition parameter, provided by the polarized absorption spectra are presented. The results of a parametric crystal field calculation, based on the experimental data, are also analyzed.

1. Introduction

The requirement of new wavelength lasers in blue, for different applications, impulsed the research of the infrared 900-950 nm quasi-three-level $^4F_{3/2} \rightarrow {}^4I_{9/2}$ emission of Nd^{3+} in various crystals and its frequency doubling conditions. Some of the applications, such as display, necessitate low wavelengths in the $^4F_{3/2} \rightarrow {}^4I_{9/2}$ Nd^{3+} laser emission. One of the shortest wavelength reported for Nd^{3+} $^4F_{3/2} \rightarrow {}^4I_{9/2}$ lasers, i.e. ~ 900 nm, has been reported [1] in strontium lanthanum aluminates $Sr_{1-x}Nd_yLa_{x-y}Mg_xAl_{12-x}O_{19}$ (ASL: Nd) crystals.

In the $SrAl_{12}O_{19}$ hexa-aluminates crystals with uniaxial magnetoplumbite-like structure, space group P6$_3$/mmc, the divalent Sr^{2+} ions in the large cationic (*2d*) sites with D$_{3h}$ local symmetry, could be replaced the trivalent Ln^{3+} (La^{3+} and Nd^{3+}) ions. The charge compensation can be accomplished by a partial substitution of Al^{3+} with Mg^{2+} [2-3] and the Nd^{3+} content can be diluted within the limits imposed by the concentration self-quenching by the optically inert La^{3+} ions [5], obtaining the disordered $Sr_{1-x}Nd_yLa_{x-y}Mg_xAl_{12-x}O_{19}$ (ASL: Nd) crystals. The high O^{2-} coordination (12 near neighbors) of Nd^{3+} (*2d*) site and its large size determine a high energetic position of the $^4F_{3/2}$ manifold as well as a moderate crystal field splitting of $^4I_{9/2}$ manifold to avoid reabsorption.

Though the Nd^{3+} spectra in ASL have been initially interpreted in terms of a single Nd^{3+} structural center [2-6], recent high-resolution optical spectroscopy [7-9] of ASL: Nd for $0.2 \leq x \leq 0.4$, $0.05 \leq y \leq 0.15$ revealed the clear presence of two types of structural centers, C$_1$ and C$_2$. The relative proportion of the two centers is determined by the composition parameter *x*: C$_1$ dominates at high *x*, while C$_2$ has large concentrations only at low *x* values. Models for

these centers have been also proposed [8]. Based on the correlation of the spectral and structural data, improved laser emission characteristics at ~901 nm in ASL: Nd have been obtained [10] by selection of the optimal compositions and pumping conditions. However, some basic problems on the spectral characteristics, structure and symmetry of non-equivalent Nd^{3+} centers in ASL are still non-elucidated.

The purpose of this study is to obtain new data on the symmetry of one of the Nd^{3+} centers in ASL (C$_2$), provided by the polarized absorption spectra and on the crystal field strength by a parametric calculation.

2. Experiment

The $Sr_{1-x}Nd_yLa_{x-y}Mg_xAl_{12-x}O_{19}$ (ASL: Nd) crystals with $x=0.05 - 0.5$, $y=0.05$, grown by Czochralski method in iridium crucibles, were used in this study. The optical spectroscopic measurements of Nd^{3+} in ASL crystals were performed on an extended spectral range up to ~ 24000 cm^{-1}. The absorption spectra at 15 K and 300 K were measured with a set-up consisting of a tungsten halogen lamp, a GDM 1m monochromator with resolution of ~0.3 cm^{-1}, using a photon counting system with a multichannel analyzer Turbo-MCS and a helium closed cycle system for low temperatures.

3. Experimental results - polarization

The Nd^{3+} two classes of centers, C$_1$ and C$_2$ in ASL are well separated in $^4I_{9/2} \rightarrow {}^4F_{3/2}$ transition (Fig. 1a), but practically coincident in $^4I_{9/2} \rightarrow {}^2P_{1/2}$ transition (Fig. 1b). The main differences between the spectra of the two Nd^{3+} main centers reside in the composition dependence, C$_2$

center dominate at low x (≤ 0.1), C_1 center becomes prevailing at $x \geq 0.5$ and in the Stark splitting of $^4F_{3/2}$ manifold (about twice larger for C_1 center than for C_2). An additional splitting of C_2 lines was observed at very low x, suggesting the existence of two distinct C_2 type centers (C_2' and C_2'') [9].

a)

b)
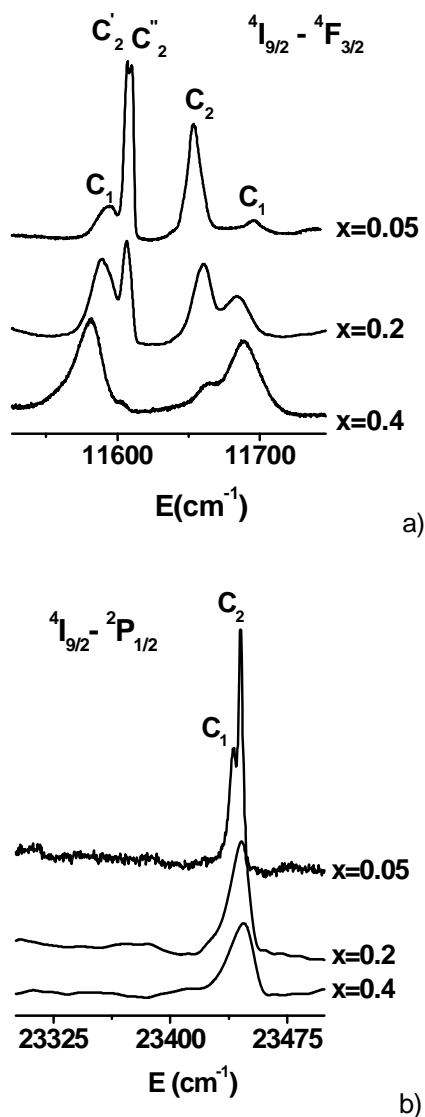
Fig. 1. The composition dependence of a) $^4I_{9/2} \rightarrow {}^4F_{3/2}$ and b) $^4I_{9/2} \rightarrow {}^2P_{1/2}$ absorption spectra of Nd^{3+} in strontium hexa-aluminate crystals at 15 K (the Nd content is y=0.05).

The polarization data could provide information on the local symmetry of a specific center. The measurements in polarized light were concentrated on the samples with $x = 0.05$ (for C_2 centers), with light propagation in the mirror (**a, b**) plane along **a** crystallographic axis, which is perpendicular on **c**, the principal axis of D_{3h} symmetry group. The measurements were performed at 15 and

300 K, the later data proved to be informative for polarization effects in transitions starting from the upper Stark levels of $^4I_{9/2}$. Generally the $\sigma (\vec{E} \perp c)$ lines are more intense than the $\pi (\vec{E} \parallel c)$ ones ($\vec{E}$ - is the electric field direction). In the $^4I_{9/2} \rightarrow {}^2P_{1/2}$ transition strong polarization effects are observed as illustrated in the 300 K absorption spectra (Fig. 2). The same is true for other transitions too, such as the $^4I_{9/2} \rightarrow {}^4F_{3/2}$, $^4F_{9/2}$ or $^2H_{11/2}$ transitions (Fig. 2). Z_i denotes the Stark components of $^4I_{9/2}$ manifold and R_i those of $^4F_{3/2}$.
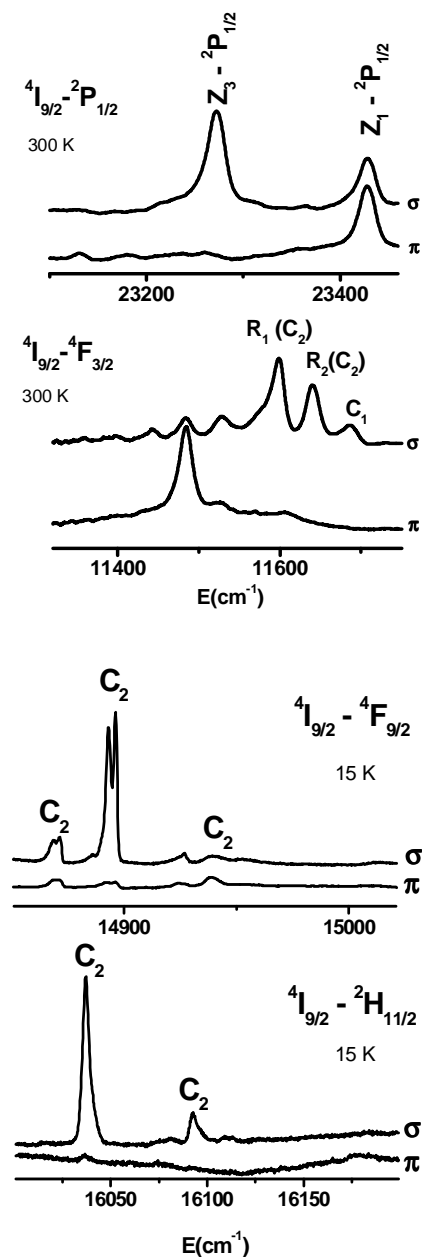
Fig. 2. The σ and π absorption spectra for several Nd^{3+} transitions in strontium hexa-aluminate of x=y=0.05 sample, $^4I_{9/2} \rightarrow {}^2P_{1/2}$, $^4I_{9/2} \rightarrow {}^4F_{3/2}$ at 300 K (left) and $^4I_{9/2} \rightarrow {}^4F_{9/2}$, $^4I_{9/2} \rightarrow {}^2H_{11/2}$ at 15 K (right).

An energy level scheme for C_2 center was obtained. The intense lines could be connected to C_2 centers due to their characteristic two line structure, but some small lines belonging to C_1 center are also present in the spectra (for x=y=0.05 sample). The previous energy levels scheme for the Nd^{3+} in ASL (x= y=0.03 - 0.15) [6] based on an unique center model, is in disagreement with our data for many manifolds, such as $^4I_{9/2}$, $^4F_{3/2}$, $F_{9/2}$, $^2H_{11/2}$ etc.

4. Results and discussion

Based on the spectral data and crystal structure, models for the two main Nd^{3+} centers in ASL ($Sr_{1-x}Nd_yLa_{x-y}Mg_xAl_{12-x}O_{19}$) have been proposed [8]: the Nd^{3+} ions in both cases has the same ionic environment 12 O^{2-}, the differences coming from the electric charge differences of nearby cations (Sr^{2+}, Ln^{3+}) in the six ($2d$) sites. Thus, the C_2 centers correspond to Nd^{3+} in a Sr^{2+} ($2d$) site with no nearby Ln^{3+} (Nd^{3+}, La^{3+}) ions and C_1 lines are composite lines of various structural centers of Nd^{3+} in a ($2d$) site with one up to all the six ($2d$) nearest neighbor sites occupied by Ln^{3+}. The additional splitting of C_2 lines in two components, observed at small x, has been tentatively connected with the perturbing effect of the Mg^{2+} ions that substitute Al^{3+}. It is very likely that the component $C_2^{''}$ is due to a Nd^{3+} having only Sr^{2+} and Al^{3+} ions as near neighbors and far away charge compensated with Mg^{2+}, and the lines $C_2^{'}$ to a collection of centers having Mg^{2+} as neighbors in various Al^{3+} tetrahedral sites close to Nd^{3+} [9]. The substitution of an Al^{3+} ion by a Mg^{2+} ion in the nearest coordination sphere of tetrahedral sites reduces the ideal electric charge of this sphere and its contribution to the crystal field potential. Combined with the fact that the relative concentration of Mg^{2+} to that of all Al^{3+} ions is small, the crystal field perturbation induced by Mg^{2+} is weaker than that due to Ln^{3+} ions. Indeed, the crystal field splitting of $^4F_{3/2}$ for C_2 center (at x=0.05) is ~ 50 cm^{-1} as compared with ~ 100 cm^{-1} for C_1 center. The cationic disorder can induce lowering in symmetry from D_{3h} for both centers, with much larger effects expected for C_1 center, in which case one could not speak of a definite symmetry. We shall restrain from this reason to the discussion of polarization effects to C_2 centers where the perturbation induced by disorder is weak.

The previous polarization measurements [6] have been analyzed in terms of an unique Nd^{3+} center in ASL and assuming that its local symmetry is pure D_{3h}. The samples analyzed in the present paper (x=y up to 0.05) have similar compositions to those (x=y=0.03, 0.15)

analyzed in [6], but even if C_2 center is prevailing at these compositions, the presence of the second center is clear (Fig. 1), and must be taken into account.

If the local symmetry at the Nd^{3+} ion is ideal D_{3h} with threefold axis along c, the J manifolds are split in the crystal field into $(2J+1)/2$ Stark doublets characterized by Γ_7, Γ_8 and Γ_9 irreducible representations [11,12]. The crystal field levels of some J manifolds interesting for our study are $D^{1/2} \rightarrow \Gamma_7$, $D^{3/2} \rightarrow \Gamma_7 + \Gamma_9$, $D^{9/2} \rightarrow \Gamma_7 + 2\Gamma_8 + 2\Gamma_9$. The electric –dipole selection rules for D_{3h} point group [11, 12] are presented in Table 1, with σ ($\vec{E} \perp c$) and π ($\vec{E} \parallel c$), and $\vec{E}$ - the electric field direction. For lower symmetries the selection rules relax, and for symmetries lower than C_{2v} all the transitions are electric - dipole allowed.

Table 1. Electric - dipole selection rules for Kramers ions in D_{3h} symmetry, with $\sigma(\vec{E} \perp c)$ and $\pi(\vec{E} \parallel c)$, polarizations and $\vec{E}$ - the electric field direction.

	Γ_7	Γ_8	Γ_9
Γ_7	-	σ, π	σ
Γ_8	σ, π	-	σ
Γ_9	σ	σ	π

The polarization spectra can be discussed in relation to the selection rules for the D_{3h} symmetry group. Since the $^4I_{9/2}$ (Z_1) $\rightarrow$ $^2P_{1/2}$ (Γ_7) line for C_2 center (x = y = 0.05) has similar intensity in both polarizations, the ground Stark level Z_1 of $^4I_{9/2}$ could be associated to a Γ_8 representation (Table 1). The symmetry of the ground state level could be also inferred from EPR data, since quite different g - factors are expected if Γ_7 ($g_\perp = 5g_\parallel$), Γ_9 ($g_\perp = 0$) or Γ_8 ($g_\parallel \sim 4$, $g_\perp \sim 2$) are ground states [13]. The recent EPR data for ASL: Nd (x=y=0.01), with $g_\parallel = 3.75$ and $g_\perp = 1.76$ [14], sustain the assignment of the Γ_8 representation to the ground Stark level of $^4I_{9/2}$.

The hot band structure of $^4I_{9/2} \rightarrow$ $^2P_{1/2}$ (Γ_7) polarized spectra of C_2 center (x=0.05) at 300 K (Fig. 2) could be well reproduced if the Stark levels of ground manifold $^4I_{9/2}$ are associated to irreducible representations of D_{3h} as follows: Z_1 - Γ_8, Z_2 - Γ_7, Z_3 - Γ_9, Z_4 - Γ_8, Z_5 - Γ_9. The $Z_{1,4}(\Gamma_8) \rightarrow$ $^2P_{1/2}$ (Γ_7) lines are observed in both polarizations, $^4I_{9/2}$ $Z_2(\Gamma_7) \rightarrow$ $^2P_{1/2}$ (Γ_7) is strictly forbidden and $^4I_{9/2}$ $Z_{3,5}(\Gamma_9) \rightarrow$ $^2P_{1/2}$ (Γ_7) are observed only in σ spectra. Fig. 3 presents part of the assignment of C_2 center lines for $^4I_{9/2} \rightarrow$ $^4F_{3/2}$ and $^4I_{9/2} \rightarrow$ $^2P_{1/2}$ transitions in terms of D_{3h} selection rules; f denote a strictly forbidden transition.
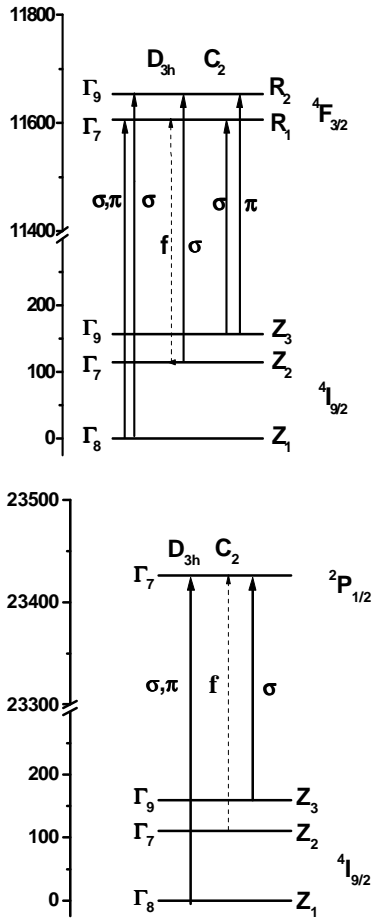
Fig. 3. The assignment of part of the Nd^{3+} $^4I_{9/2} \rightarrow {}^4F_{3/2}$ and $^4I_{9/2} \rightarrow {}^2P_{1/2}$ polarized absorption lines, at 300 K, in terms of D$_{3h}$ symmetry for C$_2$ center.

The polarization absorption data for the transitions to upper levels with $J>3/2$ for the C$_2$ center could be also interpreted in terms of D$_{3h}$ local symmetry. For example in the case of $^4I_{9/2} \rightarrow {}^4F_{9/2}$ (Γ_7, $2\Gamma_9$, $2\Gamma_8$) transition, at 15 K, for x=0.05 (Fig. 2) only three lines are present in the σ spectra of the C$_2$ centers, corresponding to the $^4I_{9/2}$ Z$_1$ (Γ_8)$\rightarrow$$^4F_{9/2}$ (Γ_7, $2\Gamma_9$) allowed transitions.

An experimental energy level scheme was assigned to C$_2$ ($C_2^{'}$) Nd^{3+} center in ASL from 15 and 300 K absorption (including polarization data) or low temperature selectively excited emission for x = y = 0.05 sample. Whereas in the $^4I_{9/2} \rightarrow {}^4F_{3/2}$ transition the lines belonging to the two centers could be clearly separated, in others ranges, especially at high energies, this division is more difficult. Parts of experimentally determined energy levels are given in Table 2. The experimental Stark levels in parentheses in Table 2 refer to small lines and their assignment is uncertain. Polarization data including hot band structure were used to assign irreducible representations to many of these levels. Significant differences between the levels assigned in this paper and those given in Table 3 of [6] are observed, not only in $^4F_{3/2}$, but in many other manifolds.

Based on the experimental energy levels for C$_2$ center given in Table 2, a crystal field calculation was performed considering the local symmetry to be D$_{3h}$. The crystal field potential corresponding to D$_{3h}$ group

$$V_{D_{3h}} = \sum_{k,q} B_q^k V_q^k \,,$$

contains only four terms, with (k=2,4,6, q=0) and (k=6, q=6). The best fit crystal field parameters are given in Table 3, and differ significantly from those given in [6]. The calculated Stark levels and their irreducible representations (I. R.) are given in Table 2. The fitting is rather good with a mean deviation of 10.5 cm^{-1} for 65 levels, the irreducible representations determined experimentally (Fig. 4) are reproduced. The estimated parameters are different from those given in Ref. [6].

Table 2. Experimental and calculated energy levels of C$_2$ center in ASL x=y=0.05, for a D$_{3h}$ local group.

$^{2S+1}L_J$	E (cm^{-1})		I. R. D$_{3h}$	$^{2S+1}L_J$	E (cm^{-1})		I. R. D$_{3h}$
	Exp.	Theor. D$_{3h}$			Exp.	Theor. D$_{3h}$	
$^4I_{9/2}$	0	-8	Γ_8	$^4F_{7/2}+$ $^4S_{3/2}$	(13520)	13538	Γ_8
	110	138	Γ_7		13567	13573	Γ_7
	155	152	Γ_9		13714	13720	Γ_9
	480	482	Γ_9		13734	13742	Γ_7
	530	529	Γ_8		13740	13750	Γ_9
					(13803)	13794	Γ_8
$^4I_{11/2}$	(2069)	2059	Γ_7	$^4F_{9/2}$	14868	14872	Γ_7
	2073	2063	Γ_9		14893	14902	Γ_9
	(2174)	2167	Γ_7		(14940)	14941	Γ_8
	(2208)	2209	Γ_9		(14952)	14958	Γ_8
	2235	2236	Γ_8		15015	14986	Γ_9
	2281	2277	Γ_8				
$^4I_{13/2}$	(3990)	3986	Γ_7	$^2H_{11/2}$	16036	16033	Γ_7
	(4084)	4085	Γ_7		16040	16046	Γ_9
	4105	4105	Γ_9		(16075)	16062	Γ_8
	(4151)	4153	Γ_7		16092	16102	Γ_9
	4185	4187	Γ_8		16110	16107	Γ_7
	4266	4266	Γ_9		(16176)	16168	Γ_8
	4377	4384	Γ_8				
$^4F_{3/2}$	11606	11583	Γ_7	$^4G_{5/2}+$ $^2G_{7/2}$	17298	17305	Γ_9
					-	17324	Γ_8
	11654	11651	Γ_9		17342	17368	Γ_7
					17465	17490	Γ_9
$^4F_{5/2}+$ $^2H_{9/2}$	(12600)	12610	Γ_8		17538	17554	Γ_7
	12639	12635	Γ_7		(17557)	17555	Γ_8
	12648	12644	Γ_9		(17575)	17578	Γ_8
	12689	12668	Γ_9				
	12703	12705	Γ_8	$^2P_{1/2}$	23427	23422	Γ_7
	12845	12861	Γ_7				
	-	12880	Γ_9				
	(12972)	12990	Γ_8				

Table 3. The estimated crystal field parameters for Nd^{3+} C_2 center in ASN (x=0.05) assuming D_{3h} .

Parameter	Value (cm^{-1})
	D_{3h}
B_0^2	516.6
B_0^4	464.8
B_0^6	-1611
B_6^6	1145
Mean deviation	10.5 for 65 levels.

The data show that the lowering in symmetry in the case of C_2 center, due to the Mg^{2+} charge compensation is small, as the polarization data that satisfy the selection rules of D_{3h} symmetry and the crystal field calculation show.

The polarization data for C_1 center (prevailing in the sample x=0.5) do not follow the selection rules for D_{3h} local symmetry. This fact can be connected to the strong cationic disorder effects leading to a lowering in local symmetry.

4. Conclusions

There were analyzed the crystal field levels and polarization data focused mainly on one of the main Nd^{3+} centers in ASL ($Sr_{1-x}Nd_yLa_{x-y}Mg_xAl_{12-x}O_{19}$), C_2 - prevailing at low x parameters, were analyzed. The polarization data suggest that the local symmetry for this center is very close to D_{3h}. The crystal field analysis based on an experimental energy level scheme for C_2 center sustains this supposition.

References

[1] G. Aka, E. Reino, D. Vivien, F. Balembois, P. Georges, B. Ferrand, OSA Trends in Optics and Photonics **68**, 329 (2002).

[2] S. Alablanche, R. Collongues, M. Leduc, A. Minvielle, J. Thery, D. Vivien, J. de Phys. IV, **1, C7**-275 (1991).

[3] S. Alablanche, A. Kahn-Harari, J. Thery, B. Viana, D. Vivien, J. Dexpert-Ghys, M. Faucher, J. Solid State Chem. **98**, 105 (1992).

[4] V. Delacarte, J. Thery, J. M. Benitez, D. Vivien, C. Borel, R. Templier, C. Wyon, OSA Proc. Adv. Solid State Lasers **24**, 123, (1995).

[5] V. Delacarte, J. Thery, D. Vivien, J. Luminescence **62**, 237, (1994).

[6] H. R. Verdun, D. E. Wortman, C. A. Morrison, J. L. Bradshaw, Optical Materials **7**, 117 (1997).

[7] D. Vivien, G. Aka, A. Lupei, V. Lupei, C. Gheorghe, Proc. SPI*E,* vol. **5581**, 287 (2004).

[8] A. Lupei, V. Lupei, C. Gheorghe, D. Vivien, G. Aka, P. Aschehoug, J. Appl. Phys. **96**(6), 3057, (2004).

[9] A. Lupei, V. Lupei, C. Gheorghe, L. Gheorghe, D. Vivien, G. Aka, Phys. Stat. Sol (c) 2(1), 276 (2005).

[10] G. Aka, D. Vivien, V. Lupei, Appl. Phys. Lett. **85**, 2685 (2004).

[11] G. F. Koster, J. O. Dimmock, R. G. Wheeler, H. Statz, Properties of the thirty-two point groups (MIT 1963).

[12] S. Hufner, Optical Spectra of Transparent Rare earth Compounds, (Academic Press, 1978).

[13] A. Abragam, B. Bleaney, Electron Paramagnetic resonance of Transition Ions (Clarendon Press, Oxford 1970).

[14] O. Guillot-Noel, Ph. Goldner, P. Higel, D. Gourier, Chem. Phys. Lett. **380**, 563 (2003).

_____
[*]Corresponding author: vlupei@pluto.infim.ro